HHS Public Access

Author manuscript

J Magn Reson Imaging. Author manuscript; available in PMC 2023 May 01.

Published in final edited form as:

J Magn Reson Imaging. 2022 May ; 55(5): 1551–1558. doi:10.1002/jmri.27965.

Imaging blood-brain barrier permeability through MRI in pediatric sickle cell disease: a feasibility study

Zixuan Lin, Ph.D.[1], **Eboni Lance, M.D., Ph.D.**[2,3], **Tiffany McIntyre, B.S.**[2], **Yang Li, Ph.D.**[1], **Peiying Liu, Ph.D.**[1], **Chantelle Lim, B.S.**[1,4], **Hongli Fan, B.S.**[1,4], **Aylin Tekes, M.D.**[1], **Alicia Cannon, Ph.D.**[5], **James F. Casella, M.D.**[6], **Hanzhang Lu, Ph.D.**[1,4,7]

[1]The Russell H. Morgan Department of Radiology & Radiological Science, Johns Hopkins University School of Medicine, Baltimore, MD 21287

[2]Department of Neurology and Developmental Medicine, Kennedy Krieger Institute, Baltimore, MD 21287

[3]Department of Neurology, Johns Hopkins University School of Medicine, Baltimore, MD 21287

[4]Department of Biomedical Engineering, Johns Hopkins University School of Medicine, Baltimore, MD 21287

[5]Department of Neuropsychology, Kennedy Krieger Institute, Baltimore, MD 21287

[6]Department of Pediatrics, Division of Hematology, Johns Hopkins University School of Medicine, Baltimore, MD 21287, Baltimore, MD 21287

[7]F. M. Kirby Research Center for Functional Brain Imaging, Kennedy Krieger Research Institute, Baltimore, MD 21287

Abstract

Background—Blood-brain barrier (BBB) disruption may lead to endothelium dysfunction and inflammation in sickle cell disease (SCD). However, abnormalities of BBB in SCD, especially in pediatric patients for whom contrast agent administration less than optimal, have not been fully characterized.

Purpose—To examine BBB permeability to water in a group of pediatric SCD participants using a non-invasive MRI technique. We hypothesized that SCD participants will have increased BBB permeability.

Study Type—Prospective cross-sectional.

Population—26 pediatric participants (10±1 years, 15F/11M) were enrolled, including 21 SCD participants and 5 sickle cell trait (SCT) participants, who were siblings of SCD patients.

Field Strength/Sequence—3T. Water-extraction-with-phase-contrast-arterial-spin-tagging (WEPCAST) with echo-planer imaging, phase-contrast and T_1-weighted magnetization-prepared-rapid-acquisition-of-gradient-echo (MPRAGE).

Corresponding author: Hanzhang Lu, Ph.D., The Russell H. Morgan Department of Radiology and Radiological Science, Johns Hopkins University School of Medicine, 600 N. Wolfe Street, Park 322, Baltimore, MD 21287, Phone: 410-955-1431 Fax: 410-614-1977, hanzhang.lu@jhu.edu.

Assessment—Water extraction fraction (E), BBB permeability-surface area product (PS), cerebral blood flow (CBF), hematological measures (hemoglobin, hematocrit, hemoglobin S), neuropsychological scores (including domains of intellectual ability, attention and executive function, academic achievement and adaptive function, and a composite score). ROIs were drawn by Z.L. (6 years of experience).

Statistical Tests—Wilcoxon rank sum test and chi-square test for group comparison of demographics. Multiple linear regression analysis of PS with diagnostic category (SCD or SCT), hematological measures and neuropsychological scores. A two-tailed *p* value of 0.05 or less was considered statistically significant.

Results—Compared with SCT participants, SCD participants had a significantly higher BBB permeability to water (SCD: 207.0±33.3mL/100g/min, SCT: 171.2±27.2mL/100g/min,). SCD participants with typically more severe phenotypes also had a significantly leakier BBB than those with typically milder phenotypes (severe: 217.3±31.7mL/100g/min, mild: 193.3±31.8mL/100g/min,). Furthermore, more severe BBB disruption was associated with worse hematological symptoms, including lower hemoglobin concentrations (β=−8.84, 95% CI [−14.69, −3.00]), lower hematocrits (β=−2.96, 95% CI [−4.84, −1.08]), and higher hemoglobin S fraction (β=0.77, 95% CI [0.014, 1.53]).

Data Conclusion—These findings support a potential role for BBB dysfunction in SCD pathogenesis of ischemic injury.

Keywords

Blood-brain barrier; sickle cell disease; WEPCAST MRI; water exchange; pediatric

Introduction

Sickle cell disease (SCD) comprises of a group of inherited red blood cell (RBC) disorders, in which mutation of the beta globin gene results in an altered beta globin protein, referred to as hemoglobin S (HbS)(1). Deoxygenated HbS molecules can form polymers, leading to deformation of RBCs into a sickled shape, which leads to hemolysis, anemia, endothelial damage and dysfunction, and vaso-occlusion (1). SCD has been associated with cerebral vasculopathy, including overt stroke or silent cerebral infarcts (2). Elevated cerebral blood flow (CBF) and velocity, reduced cerebrovascular reserve, and altered oxygen extraction have been observed in SCD patients compared with healthy controls (3–8). Among pediatric SCD patients, neurodevelopmental disorders have also been reported (9,10). Despite these observations, the exact mechanisms by which cerebral vasculopathy occurs is not well understood; in particular, there is a scarcity of literature on the structural integrity of microvasculature in SCD patients.

In SCD, vascular endothelia are exposed to cell-free hemoglobin (Hb), which can trigger the activation of these endothelial cells and result in an increased expression of adhesion molecules and an excessive inflammatory response (11). This endothelial damage has been postulated to cause disruption of membrane barriers, including the blood-brain barrier (BBB). Studies in transgenic sickle cell mice have shown an increased BBB permeability when compared to wild-type mice (12,13). This disruption in endothelium may result in

an increase in the extravasation of blood water, independent of the aquaporin-4 status on astrocyte endfeet, as the exchanged water can enter perivascular space or interstitial fluid.

Few studies have investigated the role of BBB in human SCD patients, potentially due to technical challenges in BBB assessment. Measurement of BBB permeability with dynamic contrast enhanced (DCE) MRI involves the administration of hypertonic contrast-agent, e.g. gadolinium, which has been suggested to potentiate the alignment of sickled erythrocyte inside the microvasculature and thereby increase the risk of vaso-occlusive crisis (14). Hypertonic contrast agents could also dehydrate cells and increase the chance of sickling (15). Thus, gadolinium-based MRI has rarely been used in studies of SCD, especially in the pediatric population.

Recently, there is an increasing interest in using water as an endogenous tracer to probe the BBB function. A number of non-invasive MRI techniques have been developed to measure the BBB permeability to water molecules, by labeling the water spins arterially and measuring water exchange across the BBB (16–23). Water-extraction-with-phase-contrast-arterial-spin-tagging (WEPCAST) MRI is one of these arterial-spin-labeling (ASL) based techniques which can quantify BBB permeability to water without using any contrast agent (17). It selectively measures the ASL signal at venous side at a long post-labeling delay (PLD) (3500ms used in young adults and 4000ms used in older adults) and give quantification of water extraction (24,25). This study aimed to apply this technique to evaluate BBB function in a group of pediatric SCD participants and compare it with that of participants with sickle cell trait (SCT) who were all siblings of SCD patients.

Materials and Methods

Participants

The Institutional Review Board (IRB) of Johns Hopkins University approved the study and the guardians of the participants signed IRB-approved consent forms before enrolling in the study. A total of 26 participants were enrolled. The inclusion criteria are 8 to 12 years of age with diagnosis of SCD validated by lab testing or confirmed by hematologist. Participants with any prior history of stroke, silent cerebral infarction or seizures, participants who need an interpreter, and participants who were adopted or in foster care were excluded. The study recruitment started from May 2018 and ended in May 2021.

MRI experiments

All participants were studied on a 3T Philips Ingenia System (Philips Healthcare, Best, The Netherlands). BBB permeability to water was assessed with WEPCAST MRI (17,24). Briefly, water spins are labelled on the arterial side by pseudo-continuous ASL, after which exchange occurs with the non-labeled spins in the tissue at the level of the capillary bed. The non-extracted labeled spins are selectively measured on the venous side by the WEPCAST MRI. Region of interest (ROI) of the superior sagittal sinus (SSS) was drawn manually (by Z.L. with 6 years of experience), and the WEPCAST signal at the SSS was used to quantify the extraction fraction of water (E), which together with the cerebral blood flow (*f*), can give

the BBB permeability-surface area product (PS) value, as an index of the BBB permeability to water:

$$PS = -\ln(1 - E) \cdot f \quad [1]$$

WEPCAST MRI was performed in mid-sagittal plane with a labeling duration of 2000ms (Figure 1a). A PLD of 3000ms was used. Other scanning parameters were as follows: single-shot gradient echo planar imaging readout, field of view (FOV) = 200×200mm^2, single slice, matrix = 64×64, voxel size = 3.13×3.13mm^2, slice thickness = 10mm, sensitivity encoding (SENSE) factor = 2, flip angle = 90°, encoding velocity (V_{enc}) =15cm/s, repetition time (TR) = 6250ms, echo time (TE) = 14ms, number of control/label pairs = 10, scan duration = 4min16s. An additional M_0 image with the same TE and V_{enc} and TR = 10s was acquired for normalization.

Global CBF was measured with phase-contrast (PC) MRI. An angiogram covering the cervical regions was first conducted to visualize the four feeding arteries (left and right internal carotid arteries, left and right vertebral arteries), with the following parameters: TR=26ms, TE=5.8ms, flip angle=20°, FOV=200×200×80mm^3, voxel size=0.5×0.99×2mm^3, number of slices=40, and scan duration=1min39s. PC MRI was then performed on those arteries based on the MIP of the angiogram with the imaging plane perpendicular to the targeting artery. The imaging parameters were as follows: TR=18.9ms, TE=9.3ms, flip angle=15°, FOV=200×200×5mm^3, voxel size=0.5×0.5×5mm^3, single slice, V_{enc}=40cm/s, and scan duration=15s for each artery.

A T_1-weighted magnetization-prepared-rapid-acquisition-of-gradient-echo (MPRAGE) scan was acquired for brain volumetric quantification with the following parameters: TR=7.2ms, TE=3.1ms, shot interval=2150ms, inversion time (TI)=1100ms, flip angle=10°, FOV=224×224×160mm^3, voxel size=1×1×1mm^3, number of slices=160, sagittal orientation, and scan duration=2min28s.

MRI data processing

MRI data were processed using in-house MATLAB (Mathworks Inc, Natick, MA, 2016) scripts. Detailed processing of WEPCAST MRI has been detailed in Lin et al.(17,24). The processing requires an assumption on blood T_1. In this study, E and PS were computed from the WEPCAST data by assuming 1818ms for all SCD participants and 1650ms for all SCT participants, based on the data reported by Vaclavu et al. that SCD patients have a longer blood T_1 due to the lower hematocrit (Hct) but is shorter than normal blood T_1 at equivalent Hct (26). T_1 decay during the bolus arrival time of the WEPCAST signal was corrected by $e^{-(PLD+\frac{\tau}{2})/T_1}$, where τ is the labeling duration.

The T_1-MPRAGE images were segmented using an automatic processing tool, MRICloud (27) (www.MRICloud.org, Johns Hopkins University, MD) for regional and total brain volume quantification.

For PC-MRI, regions of interest (ROIs) containing the left/right internal carotid arteries and left/right vertebral arteries were drawn manually (by Z.L. with 6 years of experience) and the flux of the arteries were calculated by the sum of the velocity in the ROI (28). Then global CBF was quantified as the flux normalized by the brain volume.

Hematological assessment

Blood samples were obtained for all participants. Concentration of Hb, Hct and HbS were measured.

Neuropsychological evaluations

Neuropsychological tests were performed (by E.B. and A.C.), including the Wechsler Intelligence Scale for Children (WISC-V)(29), Conners' Continuous Performance Test (CPT-III)(30), Behavior Rating Inventory of Executive Function (BRIEF-2)(31), Kaufman Test of Educational Achievement (3rd Edition)(32), Physical and Neurological Examination for Soft Signs (PANESS)(33), and Vineland Adaptive Behavior Scales (Vineland-II)(34). The tests were divided into four domains, i.e. intellectual ability, attention and executive function, academic achievement and adaptive function. Domain scores were generated by calculating the z-scores of each test and averaging the z-scores of the tests within each domain. A composite cognitive score was also generated by the average of the four domain scores.

Statistical analysis

Potential differences in the age and education between SCD and SCT participants were examined by Wilcoxon rank sum test. Sex difference between the two groups was examined by chi-square test. Group differences in BBB indices, CBF, hematological measures, brain volume, and cognitive performance were examined using linear regression analysis in which the group assignment was an independent variable and age, sex, and education were covariates when relevant to control for the potential difference caused by those parameters.

The associations between the BBB permeability and the hematological measures were evaluated in the entire cohort using linear regression with PS as the dependent variable, hematological parameter (i.e., Hct, Hb or HbS) as the independent variable, age and sex as the covariates. Similar analyses were performed when using the SCD participant data only.

To assess the potential difference of BBB permeability among different phenotypes of SCD, participants with hemoglobin SS or hemoglobin $S\beta^0$ thalassemia (i.e., typically severe clinical presentation) were coded as 1, and participants with hemoglobin $S\beta^+$ thalassemia or hemoglobin SC (i.e., typically mild clinical presentation) were coded as 0. A linear regression analysis was then performed where the PS value was the dependent variable and phenotype index was the independent variable, with age and sex as covariates.

Finally, the association between MRI measures and cognitive performance was assessed using linear regression in which the cognitive test scores were the dependent variables (separately for cognitive composite score and four domain scores) and PS value or E or CBF was the independent variable with age, sex, and education as covariates.

In all analyses, a two-tailed *p* value of 0.05 or less was considered statistically significant. For analysis of domain cognitive scores, Bonferroni correction was performed.

Results

Demographics, brain volumes, hematological measures and cerebral blood flow

Table 1 summarized the demographic information of all participants (N=26, 9.9±1.2 years, 15F/11M). Of these, 21 had a diagnosis of SCD. The other 5 had a diagnosis of SCT based on interpretation of their hemoglobinopathy panel by a hematologist or pathologist. Of the SCD participants, 11 had hemoglobin SS, 1 had hemoglobin $S\beta^0$ thalassemia, 3 had hemoglobin $S\beta^+$ thalassemia and 6 had hemoglobin SC. Fourteen of the SCD participants received hydroxyurea treatment previously. The SCT participants were all siblings of SCD patients. There were no statistically significant differences between SCD and SCT groups in terms of age (p=0.92), sex (p=0.19) or education (p=0.16). After controlling for age and sex, there were no statistically significant differences in brain volumes between groups, including frontal lobe (p=0.95), parietal lobe (p=0.64), temporal lobe (p=0.24), occipital lobe (p=0.74), and the whole brain (p=0.91).

Fraction of HbS was calculated for 20 of 21 SCD participants and 4 of 5 SCT participants. The missing HbS value for the SCD participant was due to technical difficulties that the labs were unable to be processed the same day as MRI, and the missing HbS value for the SCT participant was because she had HbAC trait instead of HbAS. SCD participants had a significantly lower mean Hct (SCD: 27±5%, SCT: 38±3%,), lower Hb (SCD: 9.5±1.9g/dL, SCT: 12.7±0.8g/dL,) and higher HbS fraction (SCD: 65.2±17.0%, SCT: 35.8±3.9%,) than SCT participants. In addition, SCD participants had a significant higher CBF compared with SCT participants (Figure 2a, SCD: 115.7±25.0 mL/100g/min, SCT: 72.3±11.9 mL/100g/min,). There were no significant difference in the blood velocity of the feeding arteries between SCD and SCT participants (SCD: mean velocity = 24.1±6.0cm/s, peak velocity = 49.5±10.7cm/s; SCT: mean velocity = 21.2±4.4cm/s, peak velocity = 44.1±14.5cm/s).

BBB permeability in SCD and SCT participants

Figure 1b shows representative WEPCAST images in a SCD (11yrs, female, hemoglobin SS) and a SCT (8yrs, female) participant. Compared with the SCT subject, the SCD participant revealed significantly higher signal in the SSS ($S_{WEPCAST}$=3.09±1.03% and 1.45±0.56% in SCD and SCT participants, respectively, Figure 2b), Group-level comparisons of quantitative WEPCAST indices revealed that compared to SCT participants, SCD participants had a significantly lower water extraction fraction (SCD: 83.2±5.8%, SCT: 90.2±3.8%, , Figure 2c). SCD participants also had a significantly higher PS (SCD: 207.0±33.3mL/100g/min, SCT: 171.2±27.2mL/100g/min,) than SCT participants, after adjusting for age and sex (Figure 2d).

It was also found that, within the SCD group, participants with typically more severe phenotypes (hemoglobin SS or hemoglobin $S\beta^0$ thalassemia) had a higher PS values than those with typically milder phenotypes (hemoglobin SC or hemoglobin $S\beta^+$ thalassemia) (severe: 217.3±31.7mL/100g/min, mild: 193.3±31.8mL/100g/min,).

Relationship between BBB permeability and hematological measures

Figure 3 displays scatter plots between PS values and hematological measures. Linear regression analysis showed a significant inverse relationship between PS and Hct (β=−2.96, 95% CI [−4.84, −1.08]) and between PS and Hb concentration (β=−8.84, 95% CI [−14.69, −3.00]). Individuals with a higher HbS fraction had significantly higher PS values (β=0.77, 95% CI [0.014, 1.53]).

Analyses of these relationships among the SCD participants also showed a significant negative association between PS and Hct level (β=−2.92, 95% CI [−5.78, −0.065]) and Hb level (β=−8.00, 95% CI [−15.91, −0.10]), and a positive association between PS and HbS fraction (β=1.13, 95% CI [0.015, 2.25]).

Relationship between BBB permeability and neuropsychological performance

Cognitive scores are available in 21 SCD participants and 4 out of 5 SCT participants. No significant associations between PS or E or CBF and neuropsychological scores (either domain scores or composite scores) were found, after adjusting for age, sex, education and correcting for multiple comparisons.

Discussion

This study evaluated the role of BBB permeability to water in a group of pediatric SCD participants with a non-contrast MRI technique, WEPCAST MRI. It provided preliminary evidence that compared with age-matched SCT participants, SCD participants had a significantly higher water permeability, i.e. PS value. SCD participants with a typically more severe phenotypes also had a trend of leakier BBB than those with typically milder phenotypes. Furthermore, the extent of this elevated BBB permeability was associated with hematological hallmarks of this disease such as hemoglobin concentration, hematocrit level, as well as HbS fractions in the blood.

Altered BBB permeability has been reported in many diseases, such as stroke, Alzheimer’s disease and multiple sclerosis (16,18,19,22,25,35). Although it has been postulated that in SCD endothelia are prone to damage (1,11,36,37), there were few studies investigating BBB permeability in SCD. This is largely attributed to a scarcity of non-invasive techniques to measure BBB permeability, especially those suitable for use in pediatric patients. The recent development of non-contrast BBB methods, including WEPCAST MRI, provided a new opportunity to elucidate the potential role of BBB damage in the pathophysiology of SCD.

In this study, a higher WEPCAST signal was found in SSS of the SCD participants compared with the SCT group, indicating a lower water extraction fraction in the SCD participants. The lower E was mainly due to the high blood flow in the SCD patients. When computing quantitative PS values by combining E and CBF measures, a higher permeability in SCD patients were noted. The observations of a leaky BBB in SCD patients is consistent with findings in animal models reported by Ghosh et al. and Manci et al., which revealed an increased BBB permeability in transgenic mice of SCD when compared with wild-type mice (12,13). The study of Ghosh et al. used Evan’s blue dye and Manci et al. used fluorescent dextran as an indicator of vascular permeability. The present study suggests that, using water

molecules as endogenous tracer, one can also detect BBB disruption in SCD patients. It is noteworthy that water movement in and around capillary is also controlled by aquaporin-4 in addition to endothelium. In the event that the endothelium is disrupted but aquaporin-4 function is intact, the water molecules will exit the vessel and enter the perivascular space, and flow into the CSF space. Such scenario will still result in an alteration in venous WEPCAST signal. Thus, the WEPCAST technique is expected to primarily indicate the endothelium integrity, but not that of aquaporin-4 or astrocyte endfeet, as our technique cannot differentiate exchanged water in the interstitial fluid or perivascular space, both of which are outside the draining veins. The results in our study are also consistent with two recent reports in which SCD patients showed a venous hyperintensity in the ASL images (5,6). The authors speculated that this hyperintensity is due to a cerebrovascular shunting. The results confirmed these experimental findings, i.e., there is a strong venous ASL signal in SCD patients and the signal intensity is correlated with venous blood T_2 and oxygen extraction fraction (data not shown). However, the present study used a more quantitative assessment (by determining PS) to provide evidence of an alternative explanation; that is, the hyperintensive venous signal is primarily attributed to a higher blood flow (3,4,6,8), a longer venous T_2 (although the nature of the venous oxygenation is still under some debate)(3–5,7), and a longer blood T_1 in SCD patients (26), while the actual permeability-surface area product of BBB was increased in SCD patients.

Previous studies have suggested potential mechanisms of BBB disruption in SCD. Abnormal adhesion of the sickled red blood cells to vascular wall due to a lack of shear force and specific receptor interactions has been reported in SCD (2,38). Sickle cell adhesion activates endothelia, increasing the expression of transcription factors and inhibiting the relaxation of vessels (2,11). Recurrent episodes of occlusion and reperfusion also activate the inflammatory response (36,37) and expose the endothelia to potential damage, which may result in an increased permeability. Defects in nitric oxide metabolism, oxidant stress and coagulation activation may also play a role.

Limitations

First, while we tried to maximize the demographic match of the control cohort by enrolling only healthy children with sickle cell trait, this inclusion criterion limited the sample size of the SCT group. The COVID pandemic has also been an impediment to our recruitment. We began our study in 2018, but the enrollment was disrupted by the pandemic. More control participants should be recruited in future studies to improve the power of the analyses. In addition, we would like to point out that CBF in our SCT group (72.3±11.9mL/100g/min) was similar to that of healthy non-SCT children reported in a large cohort study (70 mL/100g/min)(39). Thus the observed differences between SCD and SCT groups in this study are likely attributed to abnormalities in the SCD patients. Second, WEPCAST MRI is a global technique, which gives the BBB permeability to water in the entire brain, but does not allow the evaluation of BBB function on a region-by-region basis. Third, from a technical point-of-view, it is noted that the assumption of blood T_1 plays an important role in the quantification of PS from the WEPCAST signal. In the present study, we considered the potential difference of T_1-Hct relationship between HbS blood and normal blood, and used a fixed blood T_1 of 1818ms for SCD participants in the quantification (26). We also tested

to calculate E and PS using Hct-dependent blood T_1 based on blood T_1 models reported (40). The results were similar to those presented in the report above (see Supplementary Information Figure S1 for the effect of Hct/blood T_1 on PS quantification). Future studies should include a direct blood T_1 measurement in each individual, so that such assumptions can be avoided.

Conclusion

This study evaluated BBB permeability to water in pediatric SCD patients with a non-contrast WEPCAST MRI technique. Increased BBB permeability was found in SCD participants in comparison to SCT participants, with more severe forms of the disease corresponding to a leakier BBB. The degree of BBB damage was related to hematological abnormalities. These findings suggest a potential role of BBB dysfunction in SCD pathogenesis.

Supplementary Material

Refer to Web version on PubMed Central for supplementary material.

Grant Support:

The work was supported by the National Institutes of Health (NIH) grant R01 AG064792, RF1 AG071515, R01 NS106711, R01 NS106702, P41 EB015909, P41 EB031771, S10 OD021648, K23 HL133455-01A1, U54 HD079123 and American Heart Association grant, 19PRE34380371.

References

1. Kassim AA, DeBaun MR. Sickle cell disease, vasculopathy, and therapeutics. Annu Rev Med. 2013;64:451–66. [PubMed: 23190149]
2. Switzer JA, Hess DC, Nichols FT, Adams RJ. Pathophysiology and treatment of stroke in sickle-cell disease: present and future. Lancet Neurol. 2006;5(6):501–12. [PubMed: 16713922]
3. Jordan LC, Gindville MC, Scott AO, et al. Non-invasive imaging of oxygen extraction fraction in adults with sickle cell anaemia. Brain. 2016;139(Pt 3):738–50. [PubMed: 26823369]
4. Bush AM, Coates TD, Wood JC. Diminished cerebral oxygen extraction and metabolic rate in sickle cell disease using T2 relaxation under spin tagging MRI. Magn Reson Med. 2018;80(1):294–303. [PubMed: 29194727]
5. Juttukonda MR, Donahue MJ, Waddle SL, et al. Reduced oxygen extraction efficiency in sickle cell anemia patients with evidence of cerebral capillary shunting. J Cereb Blood Flow Metab. 2021;41(3):546–560. [PubMed: 32281458]
6. Bush A, Chai Y, Choi SY, et al. Pseudo continuous arterial spin labeling quantification in anemic subjects with hyperemic cerebral blood flow. Magn Reson Imaging. 2018;47:137–146. [PubMed: 29229306]
7. Li W, Xu X, Liu P, et al. Quantification of whole-brain oxygenation extraction fraction and cerebral metabolic rate of oxygen consumption in adults with sickle cell anemia using individual T2 -based oxygenation calibrations. Magn Reson Med. 2020;83(3):1066–1080. [PubMed: 31483528]
8. Fields ME, Guilliams KP, Ragan DK, et al. Regional oxygen extraction predicts border zone vulnerability to stroke in sickle cell disease. Neurology. 2018;90(13):e1134–e1142. [PubMed: 29500287]
9. Lance EI, Comi AM, Johnston MV, Casella JF, Shapiro BK. Risk Factors for Attention and Behavioral Issues in Pediatric Sickle Cell Disease. Clin Pediatr (Phila). 2015;54(11):1087–93. [PubMed: 26149844]

10. Lance EI, Cannon AD, Shapiro BK, Lee L-C, Johnston MV, Casella JF. Co-Occurrence of Neurodevelopmental Disorders in Pediatric Sickle Cell Disease. Journal of Developmental & Behavioral Pediatrics. 2021;42(6)
11. Sultana C, Shen Y, Rattan V, Johnson C, Kalra VK. Interaction of Sickle Erythrocytes With Endothelial Cells in the Presence of Endothelial Cell Conditioned Medium Induces Oxidant Stress Leading to Transendothelial Migration of Monocytes. Blood. 1998;92(10):3924–3935. [PubMed: 9808586]
12. Ghosh S, Tan F, Ofori-Acquah SF. Spatiotemporal dysfunction of the vascular permeability barrier in transgenic mice with sickle cell disease. Anemia. 2012;2012:582018. [PubMed: 22778926]
13. Manci EA, Hillery CA, Bodian CA, Zhang ZG, Lutty GA, Coller BS. Pathology of Berkeley sickle cell mice: similarities and differences with human sickle cell disease. Blood. 2006;107(4):1651–8. [PubMed: 16166585]
14. Dillman JR, Ellis JH, Cohan RH, et al. Safety of gadolinium-based contrast material in sickle cell disease. J Magn Reson Imaging. 2011;34(4):917–20. [PubMed: 21769966]
15. Losco P, Nash G, Stone P, Ventre J. Comparison of the effects of radiographic contrast media on dehydration and filterability of red blood cells from donors homozygous for hemoglobin A or hemoglobin S. American Journal of Hematology. 2001;68(3):149–158. [PubMed: 11754395]
16. Dickie BR, Vandesquille M, Ulloa J, Boutin H, Parkes LM, Parker GJM. Water-exchange MRI detects subtle blood-brain barrier breakdown in Alzheimer's disease rats. Neuroimage. 2019;184:349–358. [PubMed: 30219292]
17. Lin Z, Li Y, Su P, et al. Non-contrast MR imaging of blood-brain barrier permeability to water. Magn Reson Med. 2018;80(4):1507–1520. [PubMed: 29498097]
18. Ohene Y, Harrison IF, Nahavandi P, et al. Non-invasive MRI of brain clearance pathways using multiple echo time arterial spin labelling: an aquaporin-4 study. Neuroimage. 2019;188:515–523. [PubMed: 30557661]
19. Shao X, Ma SJ, Casey M, D'Orazio L, Ringman JM, Wang DJJ. Mapping water exchange across the blood-brain barrier using 3D diffusion-prepared arterial spin labeled perfusion MRI. Magn Reson Med. 2019;81(5):3065–3079. [PubMed: 30561821]
20. Petitclerc L, Schmid S, Hirschler L, van Osch MJP. Combining T2 measurements and crusher gradients into a single ASL sequence for comparison of the measurement of water transport across the blood–brain barrier. Magnetic Resonance in Medicine. 2021;85(5):2649–2660. [PubMed: 33252152]
21. Wengler K, Bangiyev L, Canli T, Duong TQ, Schweitzer ME, He X. 3D MRI of whole-brain water permeability with intrinsic diffusivity encoding of arterial labeled spin (IDEALS). Neuroimage. 2019;189:401–414. [PubMed: 30682535]
22. Wengler K, Ha J, Syritsyna O, et al. Abnormal blood-brain barrier water exchange in chronic multiple sclerosis lesions: A preliminary study. Magn Reson Imaging. 2020;70:126–133. [PubMed: 32353529]
23. He X, Wengler K, Schweitzer ME. Diffusion sensitivity of 3D-GRASE in arterial spin labeling perfusion. Magn Reson Med. 2018;80(2):736–747. [PubMed: 29315770]
24. Lin Z, Jiang D, Liu D, et al. Non-contrast assessment of blood-brain barrier permeability to water: shorter acquisition, test-retest reproducibility, and comparison with contrast-based method. Magn Reson Med. 2021;86(1):143–156. [PubMed: 33559214]
25. Lin Z, Sur S, Liu P, et al. Blood–Brain Barrier Breakdown in Relationship to Alzheimer and Vascular Disease. Annals of Neurology. 2021;90(2):227–238. [PubMed: 34041783]
26. Václavů L, van der Land V, Heijtel DFR, et al. In Vivo T1 of Blood Measurements in Children with Sickle Cell Disease Improve Cerebral Blood Flow Quantification from Arterial Spin-Labeling MRI. American Journal of Neuroradiology. 2016;37(9):1727. [PubMed: 27231223]
27. Mori S, Wu D, Ceritoglu C, et al. MRICloud: Delivering High-Throughput MRI Neuroinformatics as Cloud-Based Software as a Service. Computing in Science & Engineering. 2016;18(5):21–35.
28. Peng SL, Su P, Wang FN, et al. Optimization of phase-contrast MRI for the quantification of whole-brain cerebral blood flow. J Magn Reson Imaging. 2015;42(4):1126–33. [PubMed: 25676350]

29. Wechsler D Wechsler Intelligence Scale for Children. Wechsler Intelligence Scale for Children. Psychological Corporation; 1949.
30. Conners CK, Sitarenios G. Conners' Continuous Performance Test (CPT). In: Kreutzer JS, DeLuca J, Caplan B, eds. Encyclopedia of Clinical Neuropsychology. Springer New York; 2011:681–683.
31. Gioia GA, Isquith PK, Guy SC, L K. BRIEF2: Behavior Rating Inventory of Executive Function. Psychological Assessment Resources. 2015;
32. Singer JK, Lichtenberger EO, Kaufman JC, Kaufman AS, Kaufman NL. The Kaufman Assessment Battery for Children—Second Edition and the Kaufman Test of Educational Achievement—Second Edition. Contemporary intellectual assessment: Theories, tests, and issues, 3rd ed. The Guilford Press; 2012:269–296.
33. Werry JS, Aman MG. The reliability and diagnostic validity of the physical and neurological examination for soft signs (PANESS). Journal of autism and childhood schizophrenia. 1976;6(3):253–262. [PubMed: 1036492]
34. Sparrow SS. Vineland Adaptive Behavior Scales. In: Kreutzer JS, DeLuca J, Caplan B, eds. Encyclopedia of Clinical Neuropsychology. Springer New York; 2011:2618–2621.
35. Abbott NJ, Patabendige AA, Dolman DE, Yusof SR, Begley DJ. Structure and function of the blood-brain barrier. Neurobiol Dis. 2010;37(1):13–25. [PubMed: 19664713]
36. Osarogiagbon UR, Choong S, Belcher JD, Vercellotti GM, Paller MS, Hebbel RP. Reperfusion injury pathophysiology in sickle transgenic mice. Blood. 2000;96(1):314–320. [PubMed: 10891467]
37. Hebbel RP, Osarogiagbon R, Kaul D. The endothelial biology of sickle cell disease: inflammation and a chronic vasculopathy. Microcirculation. 2004;11(2):129–51. [PubMed: 15280088]
38. Montes RAO, Eckman JR, Hsu LL, Wick TM. Sickle erythrocyte adherence to endothelium at low shear: Role of shear stress in propagation of vaso-occlusion. American Journal of Hematology. 2002;70(3):216–227. [PubMed: 12111767]
39. Satterthwaite TD, Shinohara RT, Wolf DH, et al. Impact of puberty on the evolution of cerebral perfusion during adolescence. Proceedings of the National Academy of Sciences. 2014;111(23):8643.
40. Lu H, Clingman C, Golay X, van Zijl PC. Determining the longitudinal relaxation time (T1) of blood at 3.0 Tesla. Magn Reson Med. 2004;52(3):679–82. [PubMed: 15334591]

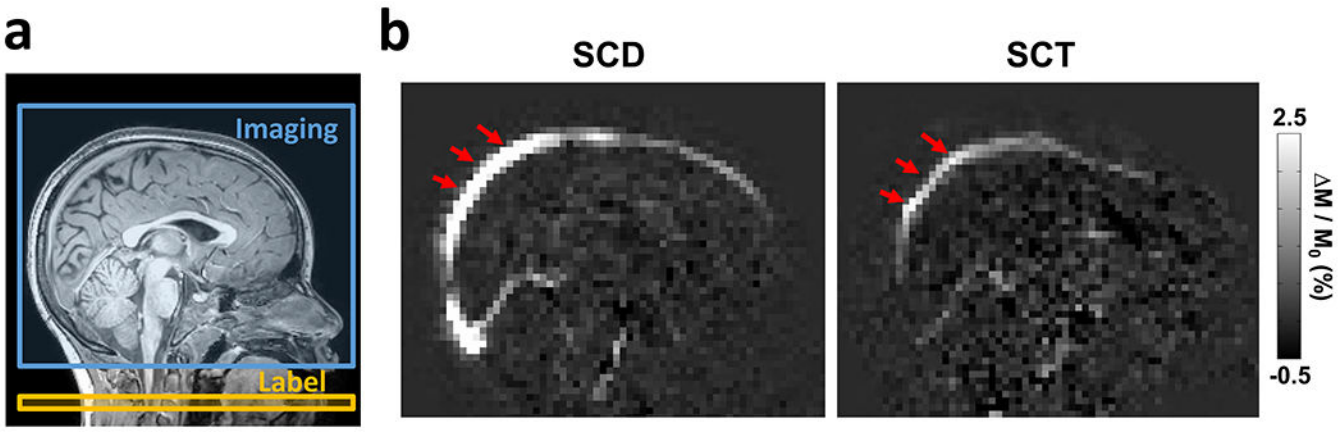

Figure 1:

WEPCAST MRI for non-contrast assessment of BBB permeability to water. (a) Typical locations of labeling (yellow) and imaging (blue) slices in WEPCAST MRI. A mid-sagittal slice is used for imaging of ASL signal in superior sagittal sinus. (b) Representative WEPCAST images from a SCD (11yrs, female, hemoglobin SS) and a SCT (8yrs, female) participant. Red arrow indicates the superior sagittal sinus.

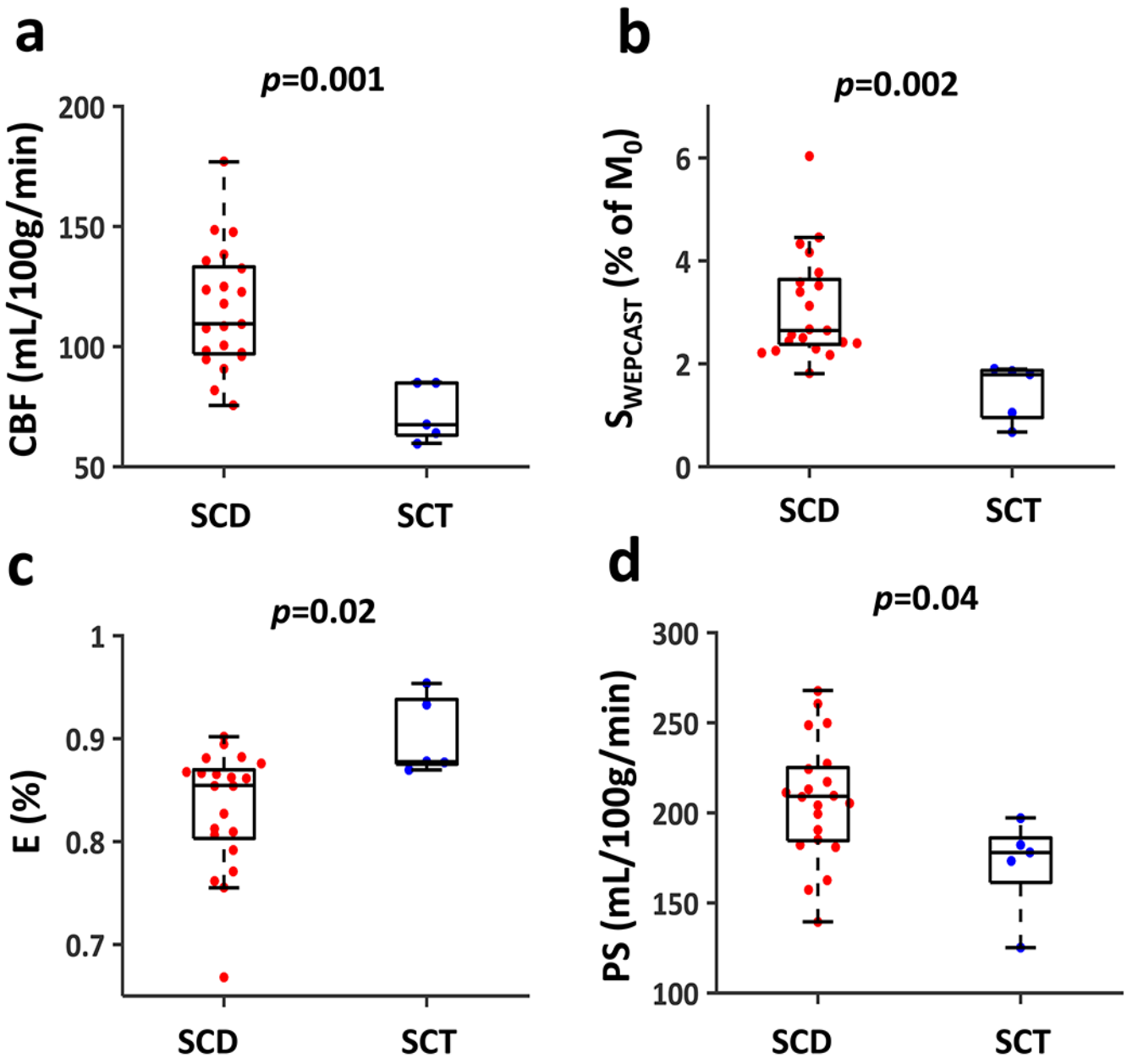

Figure 2:

Comparison of CBF, E and PS between SCD and SCT participants. (a) Boxplot of CBF comparison between SCD patients and SCT participants. (b) Boxplot of SSS WEPCAST signal in the two groups. (c) Boxplot of E in the two groups. (d) Boxplot of PS in the two groups.

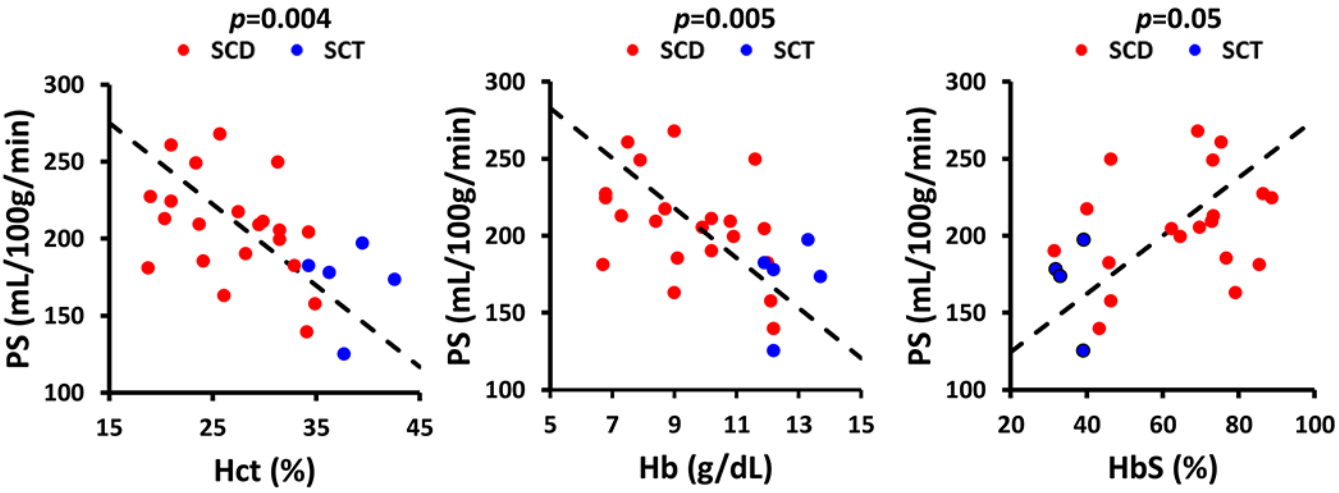

Figure 3:

Scatter plots between PS and hematological measures (Hct, Hb, and HbS level). Each dot represents data from one participant. The SCD and SCT participants are shown in different colors. The p values indicate results from linear regression after accounting for age and sex.

Table 1:

Demographics information of SCD patients and SCT participants (mean±SD)

	SCD	SCT	p-value
N	21	5	
Age, years	9.9±1.2	10.0±1.6	0.92
Females, N (%)	11 (52%)	4 (80%)	0.19
Education, years	3.6±1.2	4.6±1.5	0.16
Hematocrit (%)	27.1±5.3	38.1±3.2	**0.0004**
Hemoglobin (g/dL)	9.5±1.9	12.7±0.8	**0.002**
HbS (%)	65.2±17.0	35.8±3.9	**0.004**
CBF (mL/100g/min)	115.7±25.0	72.3±11.9	**0.001**
Intellectual ability	−0.13±0.93	0.12±0.71	0.84
Attention/Executive function	−0.083±0.70	0.62±0.56	0.55
Academic ability	−0.020±0.91	0.083±1.21	0.99
Adaptive function	0.13±0.91	−0.44±0.77	0.88
Composite score	−0.082±0.41	0.087±0.63	0.25